HHS Public Access

Author manuscript

Stem Cells. Author manuscript; available in PMC 2022 December 01.

Published in final edited form as:

Stem Cells. 2021 December ; 39(12): 1766–1777. doi:10.1002/stem.3455.

ELF3 mediates IL-1α induced differentiation of mesenchymal stem cells to inflammatory iCAFs

Linda L. Tran[1], **Truong Dang**[2], **Rintu Thomas**[2], **David R. Rowley**[2]

[1]Integrative Molecular and Biomedical Sciences Graduate Program, Baylor College of Medicine.

[2]Department of Molecular and Cellular Biology, Baylor College of Medicine, One Baylor Plaza, Houston, TX 77030, USA

Abstract

Stromal cells in the tumor microenvironment regulate the immune landscape and tumor progression. Yet, the ontogeny and heterogeneity of reactive stromal cells within tumors is not well understood. Carcinoma-associated fibroblasts exhibiting an inflammatory phenotype (iCAFs) have been identified within multiple cancers, however mechanisms that lead to their recruitment and differentiation also remain undefined. Targeting these mechanisms therapeutically may be important in managing cancer progression. Here, we identify the ELF3 transcription factor as the canonical mediator of IL-1α-induced differentiation of prostate mesenchymal stem cells to an iCAF phenotype, typical of the tumor microenvironment. Furthermore, IL-1α-induced iCAFs were subsequently refractive to TGF-β1 induced trans-differentiation to a myofibroblast phenotype (myCAF), another key carcinoma-associated fibroblast subtype typical of reactive stroma in cancer. Restricted trans-differentiation was associated with phosphorylation of the YAP protein, indicating that interplay between ELF3 action and activation of the Hippo pathway are critical for restricting trans-differentiation of iCAFs. Together, these data show that the IL-1α / ELF3 / YAP pathways are coordinate for regulating inflammatory carcinoma-associated fibroblast differentiation.

Graphical Abstract

Corresponding author: David R. Rowley, Baylor College of Medicine, One Baylor Plaza, Room 514B, Houston, TX 77030, Phone: (713) 798-6220, Fax: (713) 790-1275, drowley@bcm.edu.

Linda Tran: Conception and design, collection and/or assembly of data, data analysis and interpretation, manuscript writing, final approval of manuscript

Truong Dang: Conception and design, administrative support, collection and/or assembly of data

Rintu Thomas: Collection and/or assembly of data.

David Rowley: Conception and design, financial support, administrative support, data analysis and interpretation, manuscript writing, final approval of manuscript

The authors declare no potential conflicts of interest.

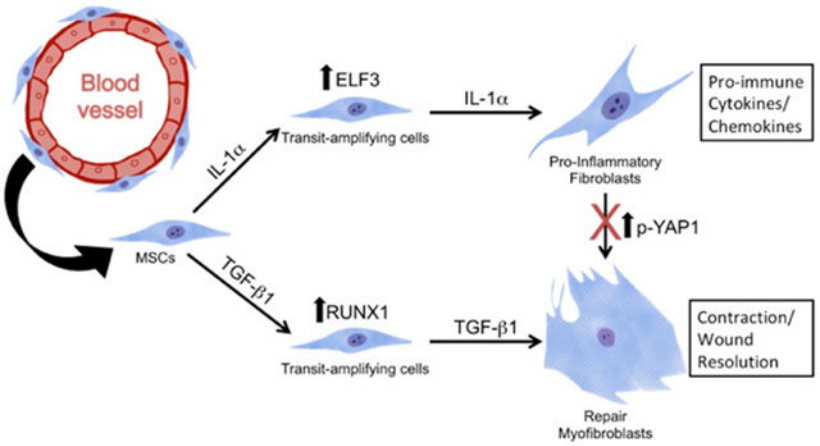

Keywords

ELF3 transcription factor; prostate cancer; pro-inflammatory fibroblast; carcinoma-associated fibroblast; tumor microenvironment; reactive stroma; Hippo pathway; interleukin 1 alpha

Introduction

Reactive stroma first appears during prostatic intraepithelial neoplasia (PIN) and co-evolves with local prostate cancer progression (1). Cancer-associated reactive stroma is composed of myofibroblasts and other stromal cell-types, collectively termed carcinoma-associated fibroblasts (CAFs) (2, 3). CAFs have been reported to be both tumor promoting and tumor-inhibiting depending on the CAF phenotype and tumor context. This has confounded attempts to effectively study the therapeutic potential of targeting CAF biology (4).
The heterogeneity of CAF phenotypes further complicates understanding their respective roles in cancer evolvability. In pancreatic cancer, both inflammatory CAFs (iCAFs) and myofibroblastic CAFs (myCAFs) have been described (5). Heterogeneity of reactive stroma CAFs is also observed in prostate cancer with approximately 50% of reactive stroma attributed to a myofibroblast myCAF phenotype (1). The classification of CAFs into distinct types is not yet well-established, as their plasticity and cell types of origin are not yet understood. However, the myCAF (contractile and matrix-secreting) and iCAF (immune modulatory) classification remains currently as a general concept.

In general, reactive stroma biology is coordinate with tissue repair biology (2). In prostate cancer, the degree of reactive stroma is predictive of biochemical recurrent disease and prostate cancer-specific death (6, 7). However, there is considerable heterogeneity in cell content and the extent of matrix remodeling in reactive stroma within a particular tumor and when compared between different tumors of the same pathological Gleason grade. Accordingly, the complex ontogeny along with mechanisms that regulate recruitment and plasticity and/or differentiation to distinct reactive stroma CAF phenotypes are not understood.

Tissue resident mesenchymal stem cells (MSCs), including pericytes, have been identified as a cell types of origin for the genesis of reactive stroma (8-10). MSCs have been identified in several postnatal tissues, including the normal human prostate gland (11, 12). Moreover, MSCs have been isolated from small and large vessels, indicating their distribution in adult tissues may be connected to their localization in the perivascular niche (13, 14). We have reported localization of CD44+/CD90+ MSCs in both the perivascular niche and stromal compartment in the normal human prostate gland and induced differentiation to myCAFs by TGF-β1 (12). Several studies show that tissue resident MSCs can differentiate to myCAFs and that TGF-β1 is a key regulatory factor in myofibroblast differentiation (12, 15, 16). Myofibroblasts function during normal tissue repair and in several disease processes with reactive stroma, including fibrosis and cancer (3, 17, 18).

Considerably less is understood about the plasticity or differentiation of iCAF subtypes. iCAFs have been identified in several cancers, including breast, ovarian, pancreatic and skin cancers (5, 19, 20). These immune-modulatory fibroblasts promote macrophage recruitment, tumor vascularization, and tumor-growth (21). While the iCAF subtype modulates inflammation, little is known about their ontogeny from MSCs or whether they result from phenotypic plasticity or a terminal differentiation. The IL-1 induced JAK/STAT mechanism has been shown to be a key inducer of the iCAF phenotype in pancreatic cancer and these studies also showed that TGF-β antagonized iCAF induction (22). These studies suggested that iCAFs and myCAFs represent interconvertible cell phenotypes. However, whether these CAF subtypes represent states of phenotypic plasticity or terminal differentiation states is not understood.

IL-1s are key upstream mediators of tissue inflammatory responses and exhibit pro-inflammatory and pro-fibrotic activities in reactive stroma (23). Inflammation is associated with poor prognosis in many cancers. It is becoming clearer that inflammation is tumor-promoting at nearly every stage of tumorigenesis including initiation, invasion, metastasis, immune evasion, and therapeutic resistance (24). IL-1α is overexpressed in epithelial cells in both benign prostatic hyperplasia and in prostate cancer (25-27). In the prostate gland, overexpression of IL-1α in the prostate epithelial cells in experimental mice, resulted in reactive stroma growth, angiogenesis, and epithelial hyperplasia (26). However, the role of IL-1α and mechanisms of action that may regulate differentiation of iCAFs from pericyte MSCs has not been investigated. Accordingly, the present study was designed to evaluate IL-1α as an inducer of MSC differentiation to iCAFs and to identify the key transcription factors that mediate IL-1α action. Furthermore, the study was designed to address whether iCAFs are restricted from TGF-β induced trans-differentiation to myCAFs and to identify key regulatory mechanisms.

We report here that IL-α overexpressing prostate epithelial cells induced differentiation of human prostate MSCs to an iCAF phenotype. Gene expression analyses and loss of function studies identified E74-like ETS transcription factor 3 (ELF3) as an essential transcription factor that mediated IL-1α induced iCAF differentiation. Furthermore, IL-1α induced iCAFs were restricted from TGF-β1-induced trans-differentiation to the myCAF phenotype. This was attributed to YAP1 phosphorylation, indicating activation of the Hippo pathway, thereby restricting SMAD activity. Perivascular cells isolated from murine microvasculature

were also responsive to IL-1α induction as compared with other tissue-resident fibroblasts. Together, these data suggest that iCAFs are a distinct subpopulation of differentiated CAFs that may originate from vascular MSC pericytes, as well as other tissue resident MSCs, following induction by IL-1α and subsequent regulation by the ELF3 transcription factor.

Results

IL-1α induces hpMSCs to an iCAF phenotype.

We have previously generated CD44+/CD90+ human prostate mesenchymal stem cells (hpMSCs) and used these to dissect mechanisms responsible for CAF differentiation (12). This work showed that TGF-β1, via RUNX1 regulation, induced hpMSC (HPS-19I cells) transit amplification and differentiation to myCAFs. Furthermore, we reported that CD44+/CD90+ positive cells reside in prostate gland stroma and perivascular niches in vivo (12). To further assess the multipotent characteristics of hpMSCs, we sought next to assess whether IL-1α would induce a phenotypic switch of these cells to iCAFs and whether the iCAF and myCAF phenotypes were inter-convertible CAF phenotypic states.

To assess CAF differentiation and IL-1α induced gene expression in hpMSCs, human normal prostate, *CSPG4* expressing, hpMSCs (HPS-19I cells) (12) were indirectly co-cultured in bicameral Millicell insert chambers with immortalized human prostate epithelial cells (PNT1A) engineered to overexpress IL-1α (26). Microarray expression analysis showed 1216 genes up-regulated and 1231 genes down-regulated in hpMSCs by at least 1.4-fold in IL-1α conditions relative to control. Gene ontology analysis (biological processes) showed IL-1α induced enrichment of genes associated with the immune response, the inflammatory response, and neutrophil chemotaxis (Fig. 1A), typical of an iCAF phenotype (5, 22). From this analysis, we created an inflammatory gene signature for hpMSCs/iCAFs consisting of genes most highly up-regulated (from 5 to 183 fold change in the gene expression array) by IL-1α: *IL1A, IL1B*, *ELF3, IL18*, *IL6, IL8*, *CSF2, and CSF3*. This gene signature pattern was confirmed with qRT-PCR in co-cultured samples and was recapitulated in hpMSCs/iCAFs induced with recombinant IL-1α (Fig. 1B).

To determine if there is a similar gene signature in murine MSC cells, we crossed R26-stop-EYFP mice with Cspg4-cre/Esr1 mice (tamoxifen-inducible Cre recombinase under control of the murine Cspg4 promoter) to create a CSPG4-EYFP reporter mouse for generating CSPG4+ cells (pericytes). To examine CSPG4+ cells, microvascular (MV) explants were isolated from abdominal adipose and prostate tissues of Cspg4-EYFP mice and maintained in culture and were subsequently treated with recombinant IL-1α to assess phenotypic CAF states. Fluorescence microscopy confirmed the presence of CSPG4+ cells localized to MV fragments and their potential to expand (Fig. 2A). The cells derived from MV fragments were passaged and enriched for the EYFP+ population using fluorescence-assisted cell sorting (FACS). Mouse CSPG4+ enriched cells exhibit an IL-1α induced inflammatory gene expression pattern similar to IL-1α induced hpMSC cells (Fig. 2B) for many but not all the genes (such as *Elf3*) in the profile. Perivascular niche-derived cells also exhibited a more robust iCAF phenotypic response to IL-1α as compared with mouse normal prostate-derived fibroblasts. Cells isolated from Cspg4-EYFP mouse microvascular fragments exhibited significant elevation in basal expression of *Il1a*, *Il1b*, *Csf1*, *Il6*, and *Csf3*, and an elevated

IL-1α induced expression of *Il1a*, *Cxcl1*, *Csf2*, *Il6*, and *Csf3* relative to normal mouse prostate-derived fibroblasts (Fig. 2C). Of interest, basal expression *Elf3* was not elevated by IL-1α in mouse perivascular cells unlike the induction observed with human hpMSCs.

ELF3 is essential for the IL-1α induced differentiation and cell density of iCAFs.

Gene expression analyses revealed elevated expression of the E74-like ETS transcription factor 3 (ELF3) in IL-1α treated hpMSC cells. ELF3 represented the only transcription factor in the top 50 elevated genes with expression at least 10-fold over control. Accordingly, we next assessed the role of ELF3 in mediating IL-1α action via loss of function studies. *ELF3* expression was attenuated using small interfering RNA (siRNA) in hpMSC cells (HPS-19I). An 83% reduction in IL-1α-induced *ELF3* gene expression was achieved, and ELF protein was non-detectable in Western blots (Fig. 3A). Importantly, knockdown of *ELF3* in hpMSC cells resulted in a significant reduction in the IL-1α-induced iCAF gene signature set (Fig. 3B). These data indicate that MSCs with *ELF3* knockdown are not induced to the iCAF phenotype. The *ELF3* knockdown results were confirmed using an additional hpMSC cell line (HPS-33Q) isolated from a different human normal prostate donor (Supplementary Fig. 1) (12). In addition, a reduced cell density was associated with knockdown of *ELF3* expression. *ELF3* attenuated cells exhibited a reduced cell density relative to control siNC cells (Fig. 4A). Both cell counting (Fig. 4B) and MTT assays (Fig. 4C) confirmed a significant reduction in hpMSC cell numbers following siRNA knockdown of *ELF3*. These data demonstrate that the ELF3 transcription factor is essential for the IL-1α induced elevation in cell number and expression of the iCAF phenotype in hpMSCs.

IL-1α-induced iCAFs exhibit restricted response to TGF-β1.

It remains unknown whether prototypical iCAFs represent a more plastic, transient fibroblast inflammatory phenotype, capable of phenotypic transdifferentiating to other CAF subtypes or whether iCAFs are incapable of phenotype reversal. As we reported previously, hpMSCs are potently induced to myofibroblastic myCAFs by TGF-β1, as are most normal fibroblasts in culture (12, 28, 29). Moreover, induction of resident fibroblasts to myCAFs by TGF-β1 is a hallmark of the cancer-associated reactive stroma (12). Accordingly, we next assessed whether IL-1α induced iCAFs were responsive or refractive to TGF-β1-induction to myCAFs. Induction of hpMSCs (HPS-19I) with IL-1α for 24 hours resulted in cells that maintained a typical TGF-β1-induced myCAF phenotype, as evidenced by *ACTA2*, *RUNX1* and *TNC* gene expression (Fig. 5A) as we reported previously (12). In contrast, induction of hpMSC cells with IL-1α for 10 days resulted in iCAFs that were refractive to TGF-β1 induction to the myCAF phenotype, including the induction of *COL1A1* (Fig. 5B). Of interest, several TGF-β1 induced genes, such as *IL6*, *ELF3* and *TNC* (Fig. 5C) were observed, although cells maintained an inflammatory gene signature expression (*IL1B*, *IL8*, etc.) (Fig. 5D). In stark contrast to control cells, IL-1α induced iCAFs were fully refractive to TGF-β1 induction of *ACTA2* (smooth muscle alpha actin), the prototypical gene that identifies myCAF differentiation (12).

To assess potential mechanisms, we next evaluated TGF-β1 canonical pathways. IL-1α induced iCAFs revealed dysregulation of *TGFBR1*, *TGFBR2*, *SMAD4*, and *SMAD7* gene expression, each involved in canonical TGF-β signal transduction (Fig. 5E). This includes

expression dysregulation of *RUNX1* (Fig. 5B). Furthermore, immunocytochemistry staining revealed inhibition of phospho-SMAD2/3 nuclear accumulation, a key step in transcription of TGF-β regulated genes (Fig. 5F). Together, these data suggest that IL-1α induced iCAFs represent a distinct differentiated CAF cell subtype that are restricted from further TGF-β1-induction to prototypical myCAF myofibroblasts via canonical TGF-β1 signaling mechanisms. However, iCAFs remained responsive to TGF-β1, likely via non-canonical pathways.

iCAFs restricted from TGF-β1–induced myCAF trans-differentiation exhibit activated Hippo pathway.

Yes-associated protein (YAP) and transcriptional coactivator with PDZ-binding motif (TAZ) are known to regulate the activity of TGF-β-regulated SMADS (30, 31). To assess requirements for YAP activity for transcription of TGF-β mediated genes in hpMSCs / myofibroblasts, we utilized the benzoporphyrin derivative Verteporfin to inhibit the YAP-TEAD interaction to subsequently disrupt downstream targets of YAP (32). Pretreatment of hpMSCs with Verteporfin strongly reduced induction of myofibroblast differentiation markers *ACTA2* and *TNC* following TGF-β stimulation (Fig. 6A), as well as YAP and phospho-YAP protein (Fig. 6B), as compared to vehicle control. These data suggest the YAP pathway is an important regulator of TGF-β1 induced myofibroblast differentiation in hpMSCs.

Phosphorylation of YAP results in cytoplasmic sequestration of the YAP/TAZ/SMADS complex, thereby restricting transcription of TGF-β mediated genes (33). To assess whether cytoplasmic sequestration of YAP may be a mechanism that restricts TGF-β mediated myCAF trans-differentiation in IL-1α induced iCAFs, we quantified phosphorylated and total protein levels of YAP in TGF-β1 treated, Il-1α -differentiated iCAFs. A significant elevation of phospho-YAP protein (Fig. 6C), but not total YAP (Fig. 6D), was observed in iCAFs upon exposure to TGF-β. These data suggest that YAP phosphorylation and subsequent cytoplasmic sequestration of YAP interactors, is one mechanism through which IL-1α induced iCAFs are restricted from subsequent TGF-β1-induced myCAF trans-differentiation.

Discussion

Carcinoma-associated fibroblasts (CAFs) are a category of stromal cells, so termed due to their emergence and proximity to developing foci of cancer epithelial cells. There is considerable evidence that CAFs are composed of a variety of stromal cell phenotypes. Collectively, CAFs affect tumor growth and progression, although mechanisms are not understood. CAFs function to remodel the extracellular matrix, maintain juxtacrine and paracrine signaling with cancer cells, and recruit and influence immune cells to the tumor microenvironment (21, 34). Less understood is CAF ontogeny, the factors that activate them, their lineage plasticity, mechanisms that influence selection pressure, and differentiation potential. Understanding CAF biology is key to tapping the therapeutic exploitation of CAFs as regulators of tumorigenesis.

Our previous work reported that MSCs reside within both the perivascular space and stroma of normal adult human prostate gland, from which they were isolated and studied (12). We report here that human normal prostate-derived MSCs can be differentiated and/or selected to iCAFs by IL-1α and present a gene signature profile that can identify this CAF subpopulation. Notably, we show ELF3 is an essential transcription factor in mediating IL-1α-induced activation and differentiation of CSPG4+ MSCs to iCAFs. These data are consistent with several reports that suggest MSCs have tropism for being activated and expanding into reactive stroma foci in both wounds and cancer (8, 13, 14, 35-38).

Our previous work also showed that human prostate MSCs are induced to transit amplification and differentiation to prototypical myofibroblast myCAFs via the actions of TGF-β1 and the RUNX1 transcription factor (12). Myofibroblastic myCAFs are a subpopulation of CAFs generally associated with later stages of repair and have been shown to be immunosuppressive, affect wound contraction, and resolve wounds (39). In contrast to myCAF pathways, we show here that iCAF pathways involve ELF3 mediation of IL-1α action to regulate human MSC cell number and differentiation to iCAFs. ELF3 was required for both an elevation in cell density and differentiation and/or selection of cells to an iCAF differentiated phenotype. It is not yet known whether the increase in cell density is due to changes in proliferation, apoptosis or cell adhesion. These data suggest a novel pathway to target iCAFs. Importantly, our data shows that IL-1α-induced human iCAFs were also restricted from TGF-β1-induced trans-differentiation to myCAFs via inactivation of the canonical TGF-β1 signaling pathway, thereby permitting maintained expression of inflammatory markers and differentiated iCAF phenotype. The data suggests that chronic inflammatory milieus favor MSCs ontogeny towards a pro-inflammatory and differentiated iCAF. Accordingly, if this biology is recapitulated in vivo, under TGF-β rich conditions, these iCAFs would be expected to persist and continue to express immune promoting cytokines. Of interest, mouse perivascular cells exhibited a similar cytokine expression profile with IL-1α induction, however we did not see an elevation of *Elf3*. It is not yet known whether this reflects differences in perivascular cells versus MSCs or mouse versus human biology.

Our data is consistent with the proposal that fibroblasts are significant mediators of the switch between acute to chronic persistent inflammation (40). It has been proposed that similar to monocyte/macrophages, MSCs can be polarized to different phenotypes, with MSC1 cells being labeled as pro-inflammatory mediators and MSC2 cells being immunosuppressive (41). MSCs participate in regulating inflammation and repair in tissues and exhibit "immunoregulatory plasticity" whereby they can either enhance or suppress immune functions (42). Accordingly, MSCs and their derivative CAF subtypes participate in complex immune regulatory processes. It is possible that iCAFs could enhance tumor promotion through cytokine production, endothelial activation, and leukocyte recruitment. The interactions between iCAFs and myCAFs is complex and poorly understood. iCAFs may contribute to sustaining myCAF populations. Myofibroblasts are essential in resolving inflammation, producing collagen, and being contractile to effect scar formation and wound healing. Myofibroblasts then undergo apoptosis when the tissue is repaired (43). In cancer and persistent fibrotic diseases, myofibroblasts/myCAFs continue to accumulate and seemingly, resist apoptosis. One mechanism by which they are able to persist is

through evading immune surveillance (44). Pro-inflammatory cytokines such as tumor necrosis factor alpha (TNF-α) and IL-17 promote cancer cell immunosuppression through stabilization of programmed cell death-ligand 1 (PD-L1) (45, 46), culminating in T cell exhaustion (47). Myofibroblasts have also been shown to express PD-L1 and affect T cell activation and proliferation (48, 49). Taken together, these studies support the possibility that iCAF fibroblasts may support myofibroblast immune evasion through expression of inflammatory cytokines.

Another key finding of this study was that iCAFs are resistant to trans-differentiation to myCAFs via canonical TGF-β1 signaling. Activation of nuclear YAP during TGF-β stimulation is critical for the establishment and maintenance of myCAFs (50). It has been shown that the cellular localization of YAP/TAZ can mediate TGF-β signaling through sequestration of SMAD complexes. Phosphorylation and subsequent cytoplasmic retention of YAP/TAZ results in suppressed TGF-β signaling (51). We show here that iCAFs exhibit decreased nuclear phospho-SMAD2/3 and increased YAP phosphorylation in response to TGF-β1. Moreover, inhibition of YAP resulted in restricted myCAF differentiation of MSCs.

Together these data suggest that activation and differentiation of tissue-resident MSCs to reactive stroma iCAFs by IL-1α is mediated by the ELF3 transcription factor. Furthermore, a complex interplay between ELF3 and YAP/TAZ acts to restrict iCAF trans-differentiation to myCAFs through canonical TGF-β1 pathways. The data suggests that trans-differentiation plasticity between these CAF subtypes is restricted. Additional studies are required to further dissect the complex biology of iCAFs in the tumor microenvironment and mechanisms that affect their recruitment and differentiation in order to identify potential therapeutic targets for managing iCAF/myCAF biology during tumorigenesis.

Methods

Cell lines

Human prostate mesenchymal stem cell (hpMSCs) lines HPS-19I and HPS-33Q were previously isolated from normal human prostate tissue from cadaver donors and maintained in Bfs medium – high glucose DMEM (Gibco) supplemented with 5% (v/v) FBS (HyClone), 5% (v/v) NuSerum (Collaborative Research), 0.5 μg/mL testosterone, 5 μg/mL insulin, 100 U/mL penicillin, and 100 μg/mL streptomycin (Sigma) as reported previously (12). PNT1A cells engineered to either overexpress IL-1α or vector only control were provided by Dr. Michael Ittmann (Baylor College of Medicine, Houston, TX) and maintained in RPMI 1640 medium (Gibco), supplemented with 10% (v/v) FBS and 200 μg/mL geneticin (Gibco) as reported previously (26). Tramp-C1D cells were provided by Dr. Barbara Foster (Roswell Park Comprehensive Cancer Center, Buffalo, NY) and maintained in Bfs medium (52). Murine prostate stromal cells were isolated in a similar manner to hpMSCs. Briefly, fresh tissue was harvested from adult mouse prostate. Explants were cut into 1 mm^3 cubes and incubated in 24-well plates containing Bfs medium, as we have reported previously (53, 54). Cells proliferating from explants were passaged and maintained in Bfs medium.

Mice

All animal studies were performed in accordance with approved IACUC protocols AN-3801 and AN-1867 at Baylor College of Medicine. Cspg4-cre/Esr1 mice, tamoxifen-inducible Cre recombinase under control of the murine Cspg4 promoter, were purchased from Jackson Laboratory (008538). The strain of origin for these mice is C57BL/6. R26-stop-EYFP mice with a *loxP*-flanked stop codon followed by the EYFP gene inserted into the *Gt(ROSA)26Sor locus*, were provided by Dr. Li Xin (University of Washington, Dept. Urol.). The strain of origin for these mice is FVB/NJ. Cspg4-cre/Esr1 mice were crossed with R26-stop-EYFP to create a tamoxifen-inducible tracing model for Cspg4+ cells, referred to as NG2-cre/Esr1*/ R26-stop-EYFP mice (Cspg4-EYFP model). To induce EYFP expression in CSPG4+ cells, tamoxifen (T5648, Sigma-Aldrich) was dissolved in 100% ethanol and diluted in corn oil to 10 mg/ml. 100 μl was administered intraperitoneally to adult mice (8-10 weeks of age) for 5 consecutive days.

Microvasculature explants

Microvasculature explants were isolated as previously described (55). Briefly, abdominal adipose and prostate tissues were isolated from tamoxifen induced Cspg4-EYFP mice and rinsed in cold DPBS. Tissue was cut into 1 mm^3 cubes and digested in high glucose DMEM supplemented with 2 mg/ml bovine serum albumin and 2 mg/ml Collagenase Type I (LS004196, Worthington) with agitation at 37°C for 30-60 minutes. Digested tissue solution was pelleted at 1000 xg for 5 minutes, washed with Bfs medium, and resuspended in Bfs medium. Suspension was filtered through sterile 300 μm nylon mesh to remove undigested tissue. Filtered solution was applied to sterile 30 μm nylon mesh to separate microvasculature fragments. Microvasculature fragments were washed from nylon mesh with Bfs medium and maintained in culture. Cells were expanded and enriched for CSPG4 through fluorescence-assisted cell sorting (FACS) to enrich for EYFP+ cells using a BD FACS Aria (Cytometry and Cell Sorting Core, Baylor College of Medicine).

Indirect co-culture

5 x 10^4 hpMSCs were seeded into 24-well plates and 2 x 10^5 engineered PNT1A cells were seeded into the upper chamber of 12 mm Millicell Cell Culture Inserts (HA mixed cellulose esters, PIHA01250, Millipore) in separate plates in their own respective mediums (listed above), as we have reported previously (12). After 24 hours, the inserts (with PNT1A cultures) were placed into a well (with hpMSCs) and maintained for 72 hours in M_0 medium – MCDB 110 supplemented with ITS, 100 U/mL penicillin, and 100 μg/mL streptomycin (Sigma). RNA was harvested separately from each compartment of cells.

RNA isolation and quantitative reverse transcription polymerase chain reaction (RT-qPCR)

Cells were homogenized using QIAshredder (Qiagen) and RNA was isolated with the RNeasy Mini Kit (Qiagen). RNA was reverse transcribed with the amfiRivert cDNA Synthesis Platinum Master Mix kit (GenDEPOT) and analyzed using FastStart Universal SYBR Green Master (Rox) (Sigma-Aldrich) on the ViiA 7 (Applied Biosystems) system. Expression levels were normalized to *GAPDH*. Primer sequences are listed in Supplementary Table 1.

Microarray analysis

RNA from hpMSCs were submitted to BCM's Genomic and RNA Profiling Core and processed for gene expression analysis via the SurePrint G3 Human Gene Expression 8x60K v2 Microarray (Agilent). Dr. Chad Creighton, (Biostatistics and Informatics Shared Resource, Dan L Duncan Comprehensive Cancer Center, BCM) performed preliminary and gene ontology enrichment analysis (biological processes) of microarray data.

Small interfering RNA (siRNA) transfection

Three different siRNA constructs (ThermoFisher Scientific were evaluated in HPS-19I cells (ElF3 Silencer Select s4624). Cells were transfected with a final concentration of 50 nM siRNA using the Neon Transfection System (Invitrogen) set at 990 V, 40 ms, and 1 pulse. Cells were transfected with Silencer Select Negative Control No. 1 or ELF3 Silencer Select s4624 (ThermoFisher Scientific). Cells were resuspended in antibiotic-free Bfs medium. siRNA sequence UCCAGGUCCACGUCACUUCca (antisense), GAAGUGACGUGGACCUGGAtt (sense), produced efficient knockdown.

Cytokine treatment

1 x 10^5 hpMSCs were seeded in 6-well plates and incubated for 24 hours in Bfs medium. Cells were serum starved for 16 hours in M_{20} medium – high glucose DMEM supplemented with 0.2% bovine serum albumin, ITS, 100 U/mL penicillin, and 100 μg/mL streptomycin. Cells were treated with 5 ng/ml recombinant human IL-1α (R&D Systems) for 24 hours in M_{20} medium. For differentiation assays, cells were treated with 5 ng/ml recombinant human IL-1α for 10 days in M_{20} medium supplemented with 0.5% (v/v) FBS and 0.5% (v/v) NuSerum. Medium and recombinant protein were refreshed every 2-3 days. Cells were then treated with 50 pM recombinant porcine TGF-β (R&D Systems) for 48 hours in M_{20} medium to differentiate into myofibroblasts.

1 x 10^5 murine stromal cells were seeded in 6-well plates and incubated for 24 hours in Bfs medium. Cells were treated with 10 ng/ml recombinant human IL-1α (R&D Systems) for 24 hours in Bfs medium.

Verteporfin treatment

For YAP1 inhibition, cells were incubated with 0.25 μM Verteporfin (Cayman Chemical) diluted in dimethyl sulfoxide for 2 hours prior to cytokine treatment.

Cell Number Assays

For growth curves, 1 x 10^5 cells were seeded in T-25 flasks in Bfs medium. Medium was refreshed every 2-3 days. At time of collection, cells were trypsinized and counted by trypan blue exclusion using the TC10 Automated Cell Counter (Bio-Rad).

For MTT (3-(4,5-Dimethylthiazol-2-yl)-2,5-Diphenyltetrazolium Bromide) assays, 1 x 10^3 cells were seeded in 96-well plates in Bfs medium. Medium was refreshed every 2-3 days. At time of collection, cells were incubated with 12 mM MTT (Molecular Probes) at 37°C for 4 hours. Dimethyl sulfoxide was added, mixed thoroughly, and incubated at 37°C for 10 minutes. Absorbances were read at 540 nm.

Immunoblotting

Cells were lysed in radioimmunoprecipitation assay (RIPA) buffer and passed through a 26-gauge needle multiple times. Lysate was combined with NuPAGE LDS Sample Buffer and reducing agent β-mercaptoethanol. Samples were boiled and separated on a 4-12% Bis-Tris gel and transferred onto a PVDF membrane with the iBlot dry transfer system (Invitrogen). Blocking and washing steps were performed using proprietary reagents from the WesternBreeze kit (Invitrogen). PVDF membranes were incubated in primary antibody overnight at 4°C. The following are primary antibodies and corresponding dilutions: ESE1 (1:10,000; ab133621; Abcam), YAP1 (1:1,000; Clone 1A12; Acris), Phospho-YAP (1:1,000; D9W21; Cell Signaling), β-Actin (1:5,000; AC-15; Sigma). Membranes were then incubated in biotinylated secondary antibody for 1 hour at room temperature. This was followed by exposure to High Sensitivity Streptavidin HRP (1:2000; 21130; Thermo Fisher Scientific). Secondary antibodies are listed in Supplementary Table 2. Signal was developed with Immobilon Western Chemiluminescent HRP substrate (WBKLS0500; Millipore) and captured using Kodak Image Station 4000R. Immunoblots were quantitated using n=3 independent experiments.

Immunocytochemistry

Autoclaved 22x22 mm cover glasses (3506; Thermo Fisher Scientific) were placed into wells prior to cell seeding and cytokine treatments that were previously described. Following treatment, cells on cover glasses were fixed in 4% paraformaldehyde for 15 minutes and thoroughly washed with DPBS. Cells were permeabilized with ice-cold 100% methanol for 10 minutes at −20°C. Cells were blocked for endogenous peroxidase activity with Bloxall (SP-6000; Vector Labs) for 10 minutes. Cells were then blocked with 5% goat serum (Sigma) for 1 hour and incubated in anti-Phospho-SMAD2/3 (1:100; D27F4; Cell Signaling) primary antibody overnight at 4°C. Cells were then incubated in biotinylated goat-anti-rabbit secondary (1:500; B2770; Invitrogen) for 45 minutes at 37°C and subsequently exposed to ready-to-use peroxidase (PK-7100; Vector Labs). Color was developed using Nova Red substrate (SK-4800; Vector Labs). Micrographs were captured with a Nikon Labophot-2 microscope with Nuance software version 3.0.0.

Statistical analysis

Paired two-tailed Student's *t*-tests and two-way ANOVAs were performed to determine significance in quantified data sets. For these analyses, p-values less than 0.05 were considered significant.

Supplementary Material

Refer to Web version on PubMed Central for supplementary material.

Acknowledgements:

This project was supported by the Cytometry and Cell Sorting Core at Baylor College of Medicine with funding from the CPRIT Core Facility Support Award (CPRIT-RP180672), the NIH (CA125123 and RR024574) and the assistance of Joel M. Sederstrom.

Funding sources:

DOD DAMD W81XWH-17-1-0605, CPRIT RP140616, RP180672, NIH R01 CA221946-01, NIH P30 CA125123-10, NIH RR024574

Data Availability Statement

The authors confirm that the data supporting the findings of this study are available within the article and its supplementary materials.

References Cited:

1. Tuxhorn JA, Ayala GE, Smith MJ, Smith VC, Dang TD, Rowley DR. Reactive stroma in human prostate cancer: induction of myofibroblast phenotype and extracellular matrix remodeling. Clin Cancer Res. 2002;8(9):2912–23. PubMed PMID: 12231536. [PubMed: 12231536]
2. Barron DA, Rowley DR. The reactive stroma microenvironment and prostate cancer progression. Endocr Relat Cancer. 2012;19(6):R187–204. Epub 2012/08/30. doi: ERC-12-0085 [pii] 10.1530/ERC-12-0085. PubMed PMID: 22930558. [PubMed: 22930558]
3. Tuxhorn JA, Ayala GE, Rowley DR. Reactive stroma in prostate cancer progression. J Urol. 2001;166(6):2472–83. PubMed PMID: 11696814. [PubMed: 11696814]
4. Sahai E, Astsaturov I, Cukierman E, DeNardo DG, Egeblad M, Evans RM, Fearon D, Greten FR, Hingorani SR, Hunter T, Hynes RO, Jain RK, Janowitz T, Jorgensen C, Kimmelman AC, Kolonin MG, Maki RG, Powers RS, Pure E, Ramirez DC, Scherz-Shouval R, Sherman MH, Stewart S, Tlsty TD, Tuveson DA, Watt FM, Weaver V, Weeraratna AT, Werb Z. A framework for advancing our understanding of cancer-associated fibroblasts. Nat Rev Cancer. 2020;20(3):174–86. Epub 2020/01/26. doi: 10.1038/s41568-019-0238-1. PubMed PMID: 31980749; PMCID: PMC7046529. [PubMed: 31980749]
5. Ohlund D, Handly-Santana A, Biffi G, Elyada E, Almeida AS, Ponz-Sarvise M, Corbo V, Oni TE, Hearn SA, Lee EJ, Chio II, Hwang CI, Tiriac H, Baker LA, Engle DD, Feig C, Kultti A, Egeblad M, Fearon DT, Crawford JM, Clevers H, Park Y, Tuveson DA. Distinct populations of inflammatory fibroblasts and myofibroblasts in pancreatic cancer. J Exp Med. 2017;214(3):579–96. Epub 2017/02/25. doi: 10.1084/jem.20162024. PubMed PMID: 28232471; PMCID: PMC5339682. [PubMed: 28232471]
6. Ayala G, Tuxhorn JA, Wheeler TM, Frolov A, Scardino PT, Ohori M, Wheeler M, Spitler J, Rowley DR. Reactive stroma as a predictor of biochemical-free recurrence in prostate cancer. Clin Cancer Res. 2003;9(13):4792–801. Epub 2003/10/29. PubMed PMID: 14581350. [PubMed: 14581350]
7. Ayala GE, Muezzinoglu B, Hammerich KH, Frolov A, Liu H, Scardino PT, Li R, Sayeeduddin M, Ittmann MM, Kadmon D, Miles BJ, Wheeler TM, Rowley DR. Determining prostate cancer-specific death through quantification of stromogenic carcinoma area in prostatectomy specimens. Am J Pathol. 2011;178(1):79–87. Epub 2011/01/13. doi: S0002-9440(10)00074-X [pii] 10.1016/j.ajpath.2010.09.042. PubMed PMID: 21224046; PMCID: 3069909. [PubMed: 21224046]
8. Kidd S, Spaeth E, Dembinski JL, Dietrich M, Watson K, Klopp A, Battula VL, Weil M, Andreeff M, Marini FC. Direct evidence of mesenchymal stem cell tropism for tumor and wounding microenvironments using in vivo bioluminescent imaging. Stem Cells. 2009;27(10):2614–23. Epub 2009/08/04. doi: 10.1002/stem.187. PubMed PMID: 19650040. [PubMed: 19650040]
9. Santamaria-Martinez A, Barquinero J, Barbosa-Desongles A, Hurtado A, Pinos T, Seoane J, Poupon MF, Morote J, Reventos J, Munell F. Identification of multipotent mesenchymal stromal cells in the reactive stroma of a prostate cancer xenograft by side population analysis. Exp Cell Res. 2009;315(17):3004–13. Epub 2009/05/19. doi: S0014-4827(09)00218-3 [pii] 10.1016/j.yexcr.2009.05.007. PubMed PMID: 19447103. [PubMed: 19447103]
10. Hosaka K, Yang Y, Seki T, Fischer C, Dubey O, Fredlund E, Hartman J, Religa P, Morikawa H, Ishii Y, Sasahara M, Larsson O, Cossu G, Cao R, Lim S, Cao Y. Pericyte-fibroblast transition promotes tumor growth and metastasis. Proc Natl Acad Sci U S A. 2016;113(38):E5618–27. Epub 2016/09/09. doi: 10.1073/pnas.1608384113. PubMed PMID: 27608497; PMCID: PMC5035870. [PubMed: 27608497]

11. da Silva Meirelles L, Chagastelles PC, Nardi NB. Mesenchymal stem cells reside in virtually all post-natal organs and tissues. J Cell Sci. 2006;119(Pt 11):2204–13. doi: 10.1242/jcs.02932. PubMed PMID: 16684817. [PubMed: 16684817]
12. Kim W, Barron DA, San Martin R, Chan KS, Tran LL, Yang F, Ressler SJ, Rowley DR. RUNX1 is essential for mesenchymal stem cell proliferation and myofibroblast differentiation. Proc Natl Acad Sci U S A. 2014;111(46):16389–94. doi: 10.1073/pnas.1407097111. PubMed PMID: 25313057; PMCID: 4246299. [PubMed: 25313057]
13. Crisan M, Yap S, Casteilla L, Chen CW, Corselli M, Park TS, Andriolo G, Sun B, Zheng B, Zhang L, Norotte C, Teng PN, Traas J, Schugar R, Deasy BM, Badylak S, Buhring HJ, Giacobino JP, Lazzari L, Huard J, Peault B. A perivascular origin for mesenchymal stem cells in multiple human organs. Cell Stem Cell. 2008;3(3):301–13. doi: 10.1016/j.stem.2008.07.003. PubMed PMID: 18786417. [PubMed: 18786417]
14. da Silva Meirelles L, Sand TT, Harman RJ, Lennon DP, Caplan AI. MSC frequency correlates with blood vessel density in equine adipose tissue. Tissue engineering Part A. 2009;15(2):221–9. Epub 2008/10/14. doi: 10.1089/ten.tea.2008.0103. PubMed PMID: 18847356; PMCID: PMC2810211. [PubMed: 18847356]
15. Desmouliere A, Geinoz A, Gabbiani F, Gabbiani G. Transforming growth factor-beta 1 induces alpha-smooth muscle actin expression in granulation tissue myofibroblasts and in quiescent and growing cultured fibroblasts. J Cell Biol. 1993;122(1):103–11. PubMed PMID: 0008314838. [PubMed: 8314838]
16. Mishra PJ, Humeniuk R, Medina DJ, Alexe G, Mesirov JP, Ganesan S, Glod JW, Banerjee D. Carcinoma-associated fibroblast-like differentiation of human mesenchymal stem cells. Cancer Res. 2008;68(11):4331–9. Epub 2008/06/04. doi: 68/11/4331 [pii] 10.1158/0008-5472.CAN-08-0943. PubMed PMID: 18519693; PMCID: 2725025. [PubMed: 18519693]
17. Gabbiani G The myofibroblast in wound healing and fibrocontractive diseases. J Pathol. 2003;200(4):500–3. PubMed PMID: 12845617. [PubMed: 12845617]
18. Desmouliere A, Guyot C, Gabbiani G. The stroma reaction myofibroblast: a key player in the control of tumor cell behavior. Int J Dev Biol. 2004;48(5-6):509–17. Epub 2004/09/07. doi: 10.1387/ijdb.041802ad. PubMed PMID: 15349825. [PubMed: 15349825]
19. Erez N, Glanz S, Raz Y, Avivi C, Barshack I. Cancer associated fibroblasts express pro-inflammatory factors in human breast and ovarian tumors. Biochem Biophys Res Commun. 2013;437(3):397–402. Epub 2013/07/09. doi: 10.1016/j.bbrc.2013.06.089. PubMed PMID: 23831470. [PubMed: 23831470]
20. Katanov C, Lerrer S, Liubomirski Y, Leider-Trejo L, Meshel T, Bar J, Feniger-Barish R, Kamer I, Soria-Artzi G, Kahani H, Banerjee D, Ben-Baruch A. Regulation of the inflammatory profile of stromal cells in human breast cancer: prominent roles for TNF-alpha and the NF-kappaB pathway. Stem Cell Res Ther. 2015;6:87. Epub 2015/05/01. doi: 10.1186/s13287-015-0080-7. PubMed PMID: 25928089; PMCID: PMC4469428. [PubMed: 25928089]
21. Erez N, Truitt M, Olson P, Arron ST, Hanahan D. Cancer-Associated Fibroblasts Are Activated in Incipient Neoplasia to Orchestrate Tumor-Promoting Inflammation in an NF-kappaB-Dependent Manner. Cancer Cell. 2010;17(2):135–47. Epub 2010/02/09. doi: 10.1016/j.ccr.2009.12.041. PubMed PMID: 20138012. [PubMed: 20138012]
22. Biffi G, Oni TE, Spielman B, Hao Y, Elyada E, Park Y, Preall J, Tuveson DA. IL1-Induced JAK/STAT Signaling Is Antagonized by TGFbeta to Shape CAF Heterogeneity in Pancreatic Ductal Adenocarcinoma. Cancer Discov. 2019;9(2):282–301. Epub 2018/10/28. doi: 10.1158/2159-8290.CD-18-0710. PubMed PMID: 30366930; PMCID: PMC6368881. [PubMed: 30366930]
23. Di Paolo NC, Shayakhmetov DM. Interleukin 1alpha and the inflammatory process. Nature immunology. 2016;17(8):906–13. Epub 2016/07/21. doi: 10.1038/ni.3503. PubMed PMID: 27434011; PMCID: PMC5152572. [PubMed: 27434011]
24. Grivennikov SI, Greten FR, Karin M. Immunity, inflammation, and cancer. Cell. 2010;140(6):883–99. Epub 2010/03/23. doi: 10.1016/j.cell.2010.01.025. PubMed PMID: 20303878; PMCID: PMC2866629. [PubMed: 20303878]

25. Ricote M, Garcia-Tunon I, Bethencourt FR, Fraile B, Paniagua R, Royuela M. Interleukin-1 (IL-1alpha and IL-1beta) and its receptors (IL-1RI, IL-1RII, and IL-1Ra) in prostate carcinoma. Cancer. 2004;100(7):1388–96. doi: 10.1002/cncr.20142. PubMed PMID: 15042672. [PubMed: 15042672]
26. Vital P, Castro P, Tsang S, Ittmann M. The Senescence-Associated Secretory Phenotype Promotes Benign Prostatic Hyperplasia. Am J Pathol. 2014. doi: 10.1016/j.ajpath.2013.11.015. PubMed PMID: 24434012.
27. Giri D, Ittmann M. Interleukin-1alpha is a paracrine inducer of FGF7, a key epithelial growth factor in benign prostatic hyperplasia. Am J Pathol. 2000;157(1):249–55. PubMed PMID: 10880394. [PubMed: 10880394]
28. Gerdes MJ, Dang TD, Larsen M, Rowley DR. Transforming growth factor-beta1 induces nuclear to cytoplasmic distribution of androgen receptor and inhibits androgen response in prostate smooth muscle cells. Endocrinology. 1998;139(8):3569–77. PubMed PMID: 0009681509. [PubMed: 9681509]
29. Gerdes MJ, Larsen M, Dang TD, Ressler SJ, Tuxhorn JA, Rowley DR. Regulation of rat prostate stromal cell myodifferentiation by androgen and TGF-beta1. Prostate. 2004;58(3):299–307. PubMed PMID: 14743470. [PubMed: 14743470]
30. Beyer TA, Weiss A, Khomchuk Y, Huang K, Ogunjimi AA, Varelas X, Wrana JL. Switch enhancers interpret TGF-beta and Hippo signaling to control cell fate in human embryonic stem cells. Cell reports. 2013;5(6):1611–24. Epub 2013/12/18. doi: 10.1016/j.celrep.2013.11.021. PubMed PMID: 24332857. [PubMed: 24332857]
31. Varelas X, Sakuma R, Samavarchi-Tehrani P, Peerani R, Rao BM, Dembowy J, Yaffe MB, Zandstra PW, Wrana JL. TAZ controls Smad nucleocytoplasmic shuttling and regulates human embryonic stem-cell self-renewal. Nat Cell Biol. 2008;10(7):837–48. Epub 2008/06/24. doi: 10.1038/ncb1748. PubMed PMID: 18568018. [PubMed: 18568018]
32. Liu-Chittenden Y, Huang B, Shim JS, Chen Q, Lee SJ, Anders RA, Liu JO, Pan D. Genetic and pharmacological disruption of the TEAD-YAP complex suppresses the oncogenic activity of YAP. Genes Dev. 2012;26(12):1300–5. Epub 2012/06/09. doi: 10.1101/gad.192856.112. PubMed PMID: 22677547; PMCID: PMC3387657. [PubMed: 22677547]
33. Narimatsu M, Samavarchi-Tehrani P, Varelas X, Wrana JL. Distinct polarity cues direct Taz/Yap and TGFbeta receptor localization to differentially control TGFbeta-induced Smad signaling. Dev Cell. 2015;32(5):652–6. Epub 2015/03/12. doi: 10.1016/j.devcel.2015.02.019. PubMed PMID: 25758863. [PubMed: 25758863]
34. Nwabo Kamdje AH, Kamga PT, Simo RT, Vecchio L, Seke Etet PF, Muller JM, Bassi G, Lukong E, Goel RK, Amvene JM, Krampera M. Mesenchymal stromal cells' role in tumor microenvironment: involvement of signaling pathways. Cancer Biol Med. 2017;14(2):129–41. Epub 2017/06/14. doi: 10.20892/j.issn.2095-3941.2016.0033. PubMed PMID: 28607804; PMCID: PMC5444925. [PubMed: 28607804]
35. Corselli M, Crisan M, Murray IR, West CC, Scholes J, Codrea F, Khan N, Peault B. Identification of perivascular mesenchymal stromal/stem cells by flow cytometry. Cytometry A. 2013;83(8):714–20. Epub 2013/07/03. doi: 10.1002/cyto.a.22313. PubMed PMID: 23818229. [PubMed: 23818229]
36. Covas DT, Panepucci RA, Fontes AM, Silva WA Jr., Orellana MD, Freitas MC, Neder L, Santos AR, Peres LC, Jamur MC, Zago MA. Multipotent mesenchymal stromal cells obtained from diverse human tissues share functional properties and gene-expression profile with CD146+ perivascular cells and fibroblasts. Exp Hematol. 2008;36(5):642–54. Epub 2008/02/26. doi: 10.1016/j.exphem.2007.12.015. PubMed PMID: 18295964. [PubMed: 18295964]
37. Park TS, Gavina M, Chen CW, Sun B, Teng PN, Huard J, Deasy BM, Zimmerlin L, Peault B. Placental perivascular cells for human muscle regeneration. Stem Cells Dev. 2011;20(3):451–63. Epub 2010/10/07. doi: 10.1089/scd.2010.0354. PubMed PMID: 20923371; PMCID: PMC3120979. [PubMed: 20923371]
38. Shi S, Gronthos S. Perivascular niche of postnatal mesenchymal stem cells in human bone marrow and dental pulp. J Bone Miner Res. 2003;18(4):696–704. Epub 2003/04/04. doi: 10.1359/jbmr.2003.18.4.696. PubMed PMID: 12674330. [PubMed: 12674330]

39. Tomasek JJ, Gabbiani G, Hinz B, Chaponnier C, Brown RA. Myofibroblasts and mechano-regulation of connective tissue remodelling. Nature reviews Molecular cell biology. 2002;3(5):349–63. doi: 10.1038/nrm809. PubMed PMID: 11988769. [PubMed: 11988769]
40. Buckley CD, Pilling D, Lord JM, Akbar AN, Scheel-Toellner D, Salmon M. Fibroblasts regulate the switch from acute resolving to chronic persistent inflammation. Trends Immunol. 2001;22(4):199–204. Epub 2001/03/29. doi: 10.1016/s1471-4906(01)01863-4. PubMed PMID: 11274925. [PubMed: 11274925]
41. Waterman RS, Tomchuck SL, Henkle SL, Betancourt AM. A new mesenchymal stem cell (MSC) paradigm: polarization into a pro-inflammatory MSC1 or an Immunosuppressive MSC2 phenotype. PLoS One. 2010;5(4):e10088. Epub 2010/05/04. doi: 10.1371/journal.pone.0010088. PubMed PMID: 20436665; PMCID: 2859930. [PubMed: 20436665]
42. Wang Y, Chen X, Cao W, Shi Y. Plasticity of mesenchymal stem cells in immunomodulation: pathological and therapeutic implications. Nature immunology. 2014;15(11):1009–16. Epub 2014/10/21. doi: 10.1038/ni.3002. PubMed PMID: 25329189. [PubMed: 25329189]
43. Hinz B. Formation and function of the myofibroblast during tissue repair. J Invest Dermatol. 2007;127(3):526–37. doi: 10.1038/sj.jid.5700613. PubMed PMID: 17299435. [PubMed: 17299435]
44. Wallach-Dayan SB, Golan-Gerstl R, Breuer R. Evasion of myofibroblasts from immune surveillance: a mechanism for tissue fibrosis. Proc Natl Acad Sci U S A. 2007;104(51):20460–5. Epub 2007/12/14. doi: 10.1073/pnas.0705582104. PubMed PMID: 18077384; PMCID: PMC2154453. [PubMed: 18077384]
45. Lim SO, Li CW, Xia W, Cha JH, Chan LC, Wu Y, Chang SS, Lin WC, Hsu JM, Hsu YH, Kim T, Chang WC, Hsu JL, Yamaguchi H, Ding Q, Wang Y, Yang Y, Chen CH, Sahin AA, Yu D, Hortobagyi GN, Hung MC. Deubiquitination and Stabilization of PD-L1 by CSN5. Cancer Cell. 2016;30(6):925–39. Epub 2016/11/22. doi: 10.1016/j.ccell.2016.10.010. PubMed PMID: 27866850; PMCID: PMC5171205. [PubMed: 27866850]
46. Wang X, Yang L, Huang F, Zhang Q, Liu S, Ma L, You Z. Inflammatory cytokines IL-17 and TNF-alpha up-regulate PD-L1 expression in human prostate and colon cancer cells. Immunology letters. 2017;184:7–14. Epub 2017/02/23. doi: 10.1016/j.imlet.2017.02.006. PubMed PMID: 28223102; PMCID: PMC5362328. [PubMed: 28223102]
47. Grinberg-Bleyer Y, Ghosh S. A Novel Link between Inflammation and Cancer. Cancer Cell. 2016;30(6):829–30. Epub 2016/12/14. doi: 10.1016/j.ccell.2016.11.013. PubMed PMID: 27960080. [PubMed: 27960080]
48. Beswick EJ, Grim C, Singh A, Aguirre JE, Tafoya M, Qiu S, Rogler G, McKee R, Samedi V, Ma TY, Reyes VE, Powell DW, Pinchuk IV. Expression of Programmed Death-Ligand 1 by Human Colonic CD90(+) Stromal Cells Differs Between Ulcerative Colitis and Crohn's Disease and Determines Their Capacity to Suppress Th1 Cells. Front Immunol. 2018;9:1125. Epub 2018/06/19. doi: 10.3389/fimmu.2018.01125. PubMed PMID: 29910803; PMCID: PMC5992387. [PubMed: 29910803]
49. Pinchuk IV, Saada JI, Beswick EJ, Boya G, Qiu SM, Mifflin RC, Raju GS, Reyes VE, Powell DW. PD-1 ligand expression by human colonic myofibroblasts/fibroblasts regulates CD4+ T-cell activity. Gastroenterology. 2008;135(4):1228–37, 37 e1-2. Epub 2008/09/02. doi: 10.1053/j.gastro.2008.07.016. PubMed PMID: 18760278; PMCID: PMC2584612. [PubMed: 18760278]
50. Calvo F, Ege N, Grande-Garcia A, Hooper S, Jenkins RP, Chaudhry SI, Harrington K, Williamson P, Moeendarbary E, Charras G, Sahai E. Mechanotransduction and YAP-dependent matrix remodelling is required for the generation and maintenance of cancer-associated fibroblasts. Nat Cell Biol. 2013;15(6):637–46. Epub 2013/05/28. doi: 10.1038/ncb2756. PubMed PMID: 23708000; PMCID: PMC3836234. [PubMed: 23708000]
51. Varelas X, Samavarchi-Tehrani P, Narimatsu M, Weiss A, Cockburn K, Larsen BG, Rossant J, Wrana JL. The Crumbs complex couples cell density sensing to Hippo-dependent control of the TGF-beta-SMAD pathway. Dev Cell. 2010;19(6):831–44. Epub 2010/12/15. doi: 10.1016/j.devcel.2010.11.012. PubMed PMID: 21145499. [PubMed: 21145499]
52. Foster BA, Gingrich JR, Kwon ED, Madias C, Greenberg NM. Characterization of prostatic epithelial cell lines derived from transgenic adenocarcinoma of the mouse prostate (TRAMP) model. Cancer Res. 1997;57(16):3325–30. PubMed PMID: 9269988. [PubMed: 9269988]

53. Rowley DR. Characterization of a fetal urogenital sinus mesenchymal cell line U4F: Secretion of a negative growth regulatory activity. In Vitro CellDevBiol. 1992;28:29–38.

54. Rowley DR, Tindall DJ. Responses of NBT-II bladder carcinoma cells to conditioned medium from normal fetal urogenital sinus. Cancer Res. 1987;47:2955–60. [PubMed: 3567912]

55. San Martin R, Barron DA, Tuxhorn JA, Ressler SJ, Hayward SW, Shen X, Laucirica R, Wheeler TM, Gutierrez C, Ayala GE, Ittmann M, Rowley DR. Recruitment of CD34(+) fibroblasts in tumor-associated reactive stroma: the reactive microvasculature hypothesis. Am J Pathol. 2014;184(6):1860–70. doi: 10.1016/j.ajpath.2014.02.021. PubMed PMID: 24713391; PMCID: 4044710. [PubMed: 24713391]

Statement of Significance

The mechanisms determining the heterogeneity of stromal populations in the tumor microenvironment are poorly understood. The present study identifies ELF3 as an essential transcription factor in the differentiation of a key pro-inflammatory stromal cell type and identifies mesenchymal stem cells as a progenitor of inflammatory carcinoma-associated fibroblasts.

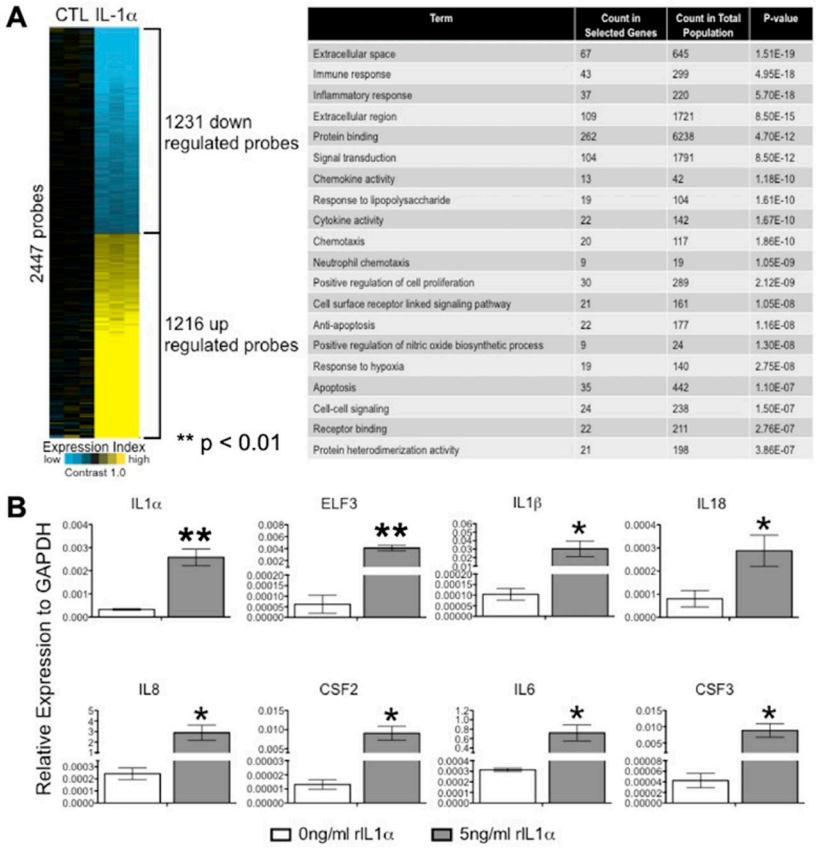

Term	Count in Selected Genes	Count in Total Population	P-value
Extracellular space	67	645	1.51E-19
Immune response	43	299	4.95E-18
Inflammatory response	37	220	5.70E-18
Extracellular region	109	1721	8.50E-15
Protein binding	262	6238	4.70E-12
Signal transduction	104	1791	8.50E-12
Chemokine activity	13	42	1.18E-10
Response to lipopolysaccharide	19	104	1.61E-10
Cytokine activity	22	142	1.67E-10
Chemotaxis	20	117	1.86E-10
Neutrophil chemotaxis	9	19	1.05E-09
Positive regulation of cell proliferation	30	289	2.12E-09
Cell surface receptor linked signaling pathway	21	161	1.05E-08
Anti-apoptosis	22	177	1.16E-08
Positive regulation of nitric oxide biosynthetic process	9	24	1.30E-08
Response to hypoxia	19	140	2.75E-08
Apoptosis	35	442	1.10E-07
Cell-cell signaling	24	238	1.50E-07
Receptor binding	22	211	2.76E-07
Protein heterodimerization activity	21	198	3.86E-07

Figure 1. IL-1α activates hpMSCs to an inflammatory phenotype.

Immortalized normal human prostate epithelial cells (PNT1A) containing the pcDNA control vector and the IL-1α overexpression vector were indirectly co-cultured human prostate mesenchymal stem cells (hpMSCs) for 72 hr. RNA was harvested from the stromal compartment and submitted for gene expression analysis (Agilent SurePrint G3 Human Gene Expression 8x60K v2 Microarray). 2447 gene probes had a significant fold change greater than 1.4 or less than 1/1.4. 1231 genes were down-regulated, and 1216 genes were up-regulated. Gene ontology analysis showed enrichment of genes associated with the immune response, the inflammatory response, and neutrophil chemotaxis (A). Treatment of hpMSCs with 5 ng/ml of recombinant human IL-1α recapitulates the inflammatory gene signature identified in the microarray (B). For (A): n = 3; $p < 0.01$ (**). For (B): data represent mean ± SEM; n = 4; $p < 0.05$ (*), $p < 0.01$ (**).

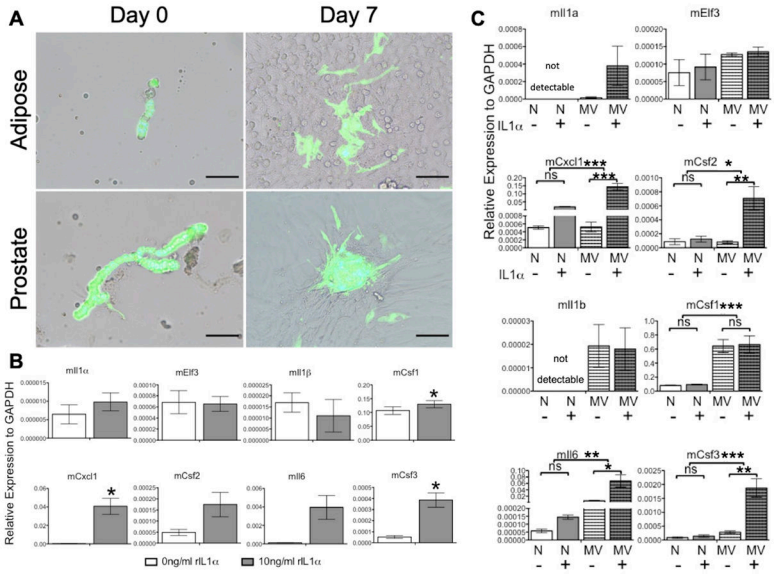

Figure 2. IL-1α activates Cspg4+ cells to an iCAF phenotype.

Microvasculature (MV) explants were isolated from abdominal adipose and prostate tissues of Cspg4-EYFP mice and maintained in culture. Fluorescence microscopy confirmed the presence of Cspg4+ cells localized to MV fragments and their potential to expand (A). Cspg4+ enriched cells from MV fragments exhibit an inflammatory profile that trends similarly to human cells when treated with 10 ng/ml of recombinant human IL-1α (B). Cells isolated from MV fragments (denoted MV) showed higher threshold and induction levels of genes associated with inflammation as compared to normal prostate fibroblasts (denoted N) (C). Note that cells isolated from MV are more responsive to inflammatory mediator IL-1α than normal fibroblasts. Data represent mean ± SEM; n = 3; $p < 0.05$ (*), $p < 0.01$ (**), $p < 0.001$ (***). ns: not significant. Scale bars = 100 μm.

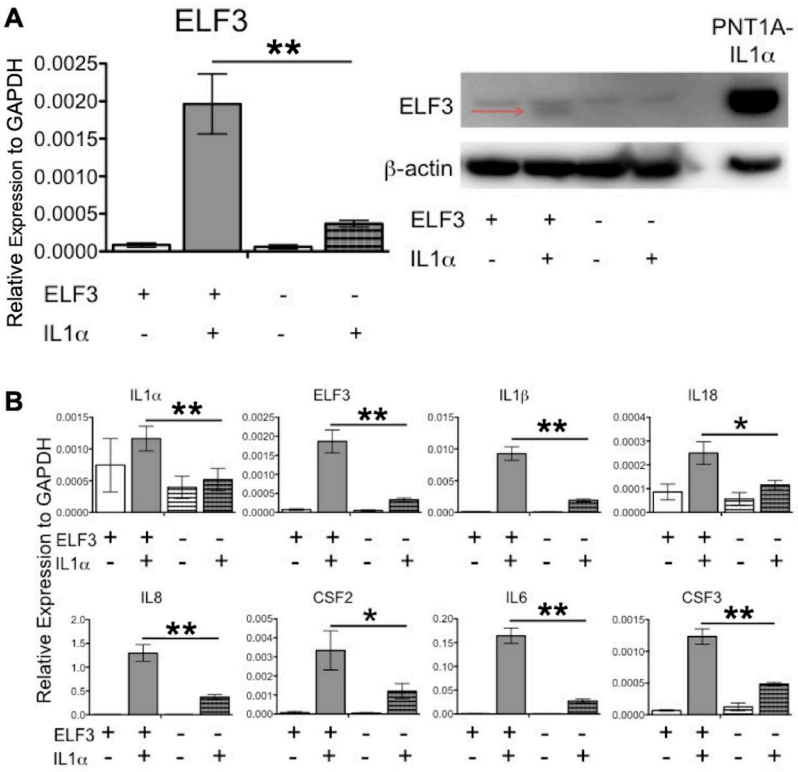

Figure 3. ELF3 is essential for the IL-1α induced inflammatory response in hpMSCs.

ELF3 siRNA efficiently knocked down gene and protein expression of ELF3 in hpMSCs. Due to low threshold levels, knockdown is much more evident in IL-1α induced conditions (denoted with red arrow) (A). Prostate epithelial cells (PNTIA) overexpressing IL-1α were used as a positive loading control (A). Silencing of *ELF3* strongly mediated IL-1α induction of inflammatory genes in hpMSCs (B). For (A): data represent mean ± SEM; n = 3; $p < 0.05$ (*). For (B): data represent mean ± SEM; n = 4; $p < 0.05$ (*), $p < 0.01$ (**).

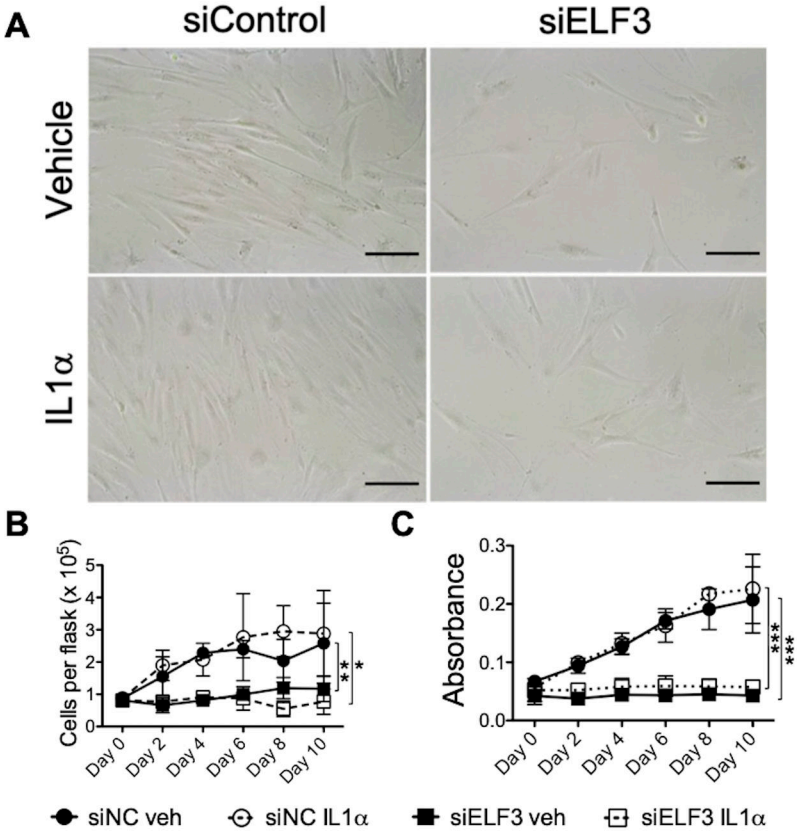

Figure 4. ELF3 is essential for increase in hpMSC cell number.

A decrease in cell number was associated with inhibition of *ELF3* in hpMSC cell cultures. By six days post transfection with negative control siRNA (siNC), hpMSCs reached nearly 100% confluency in culture. In contrast, cells transfected with ELF3 siRNA (siELF3) did not change in cell number (A). Growth curves (B) and MTT assays (C) in full serum medium following siRNA knockdown showed no significant increase in siELF3 cell count over the course of 10 days. In serum-containing conditions, IL-1α treatment appeared to have no significant effect on proliferation. Data represent mean ± SEM; n = 3; $p < 0.05$ (*), $p < 0.01$ (**), $p < 0.001$ (***). Scale bars = 100 μm

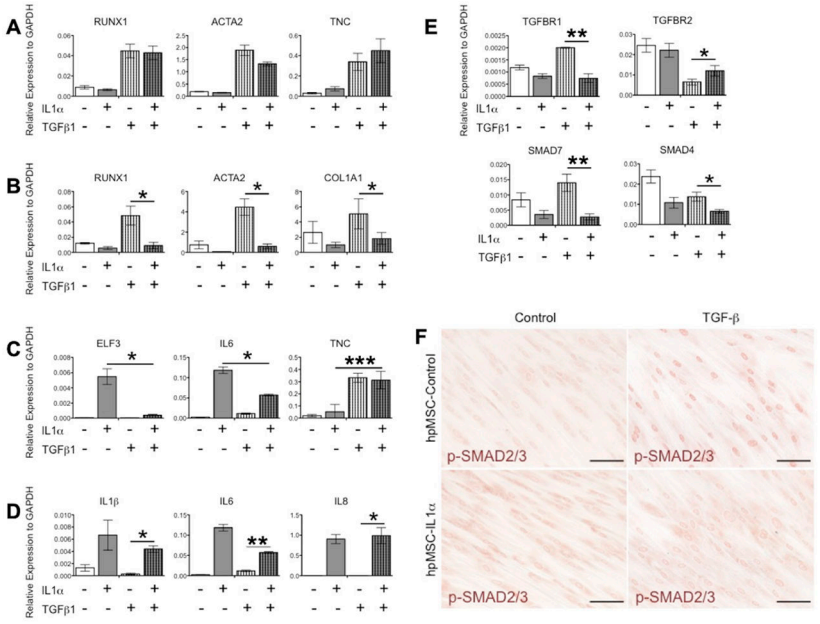

Figure 5. Chronic treatment with IL-1α induces hpMSCs to pro-inflammatory iCAFs and restricts TGF-β1 induced myCAF responses.

Acute treatment of hpMSCs with recombinant IL-1α for 24 hours resulted in cells that retained TGF-β1 induced myofibroblast differentiation as evidenced by *ACTA2* and *TNC* expression (A), while chronic IL-1α treatment for 10 days resulted in iCAFs that were restricted from differentiation to myofibroblasts (lack of *ACTA2* and *COL1A1* induction) (B), as determined by gene expression of prototypical myofibroblast markers. IL-1α induced iCAFs remain responsive to TGF-β1, as evidenced by induced gene expression including *TNC* (C), yet they continue to express interleukin inflammatory markers (D). They exhibit dysregulation of genes involved in canonical TGF-β signal transduction including *SMAD7* (E). Immunocytochemical staining revealed inhibition of phospho-SMAD2/3 nuclear accumulation, a key step in transcription of TGF-β1 regulated genes (lower right panel) (F). Data represent mean ± SEM; n = 3; $p < 0.05$ (*), $p < 0.01$ (**), $p < 0.001$ (***). Scale bars = 100 μm.

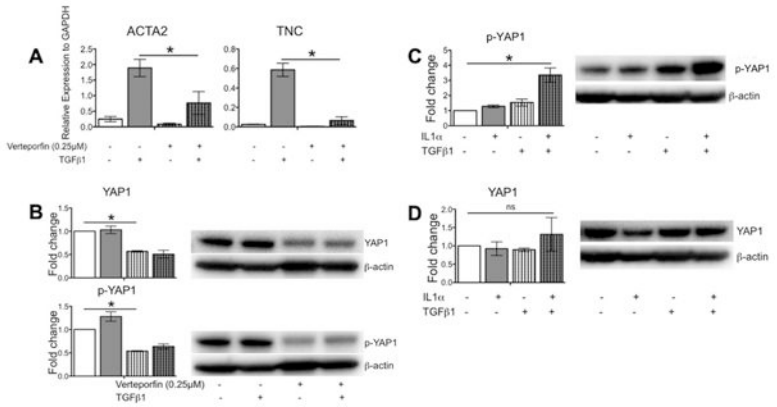

Figure 6. iCAFs activated Hippo pathway associates with restricted TGF-β1mediated myofibroblast differentiation.

Pretreatment of hpMSCs with the YAP inhibitor Verteporfin reduced TGF-β1 induced myofibroblast differentiated gene expression (A) and protein expression of YAP and phospho-YAP (B). iCAFs show a significant increase of phospho-YAP (C), but not total YAP (D), in TGF-β1 conditions. Data represent mean ± SEM; n = 3; $p < 0.05$ (*). ns: not significant.